Evaluation of surface water fluxes of the pan-Arctic land region with a land surface model and ERA-40 reanalysis

Fengge Su,[1] Jennifer C. Adam,[1] Kevin E. Trenberth,[2] and Dennis P. Lettenmaier[1]

Received 17 June 2005; revised 10 October 2005; accepted 2 December 2005; published 15 March 2006.

[1] The seasonal, spatial, and latitudinal variability of precipitation (P), evapotranspiration (E), and runoff (R) are examined for large Arctic river basins and for the entire pan-Arctic domain using a 21-year off-line simulation of the Variable Infiltration Capacity (VIC) macroscale hydrology model and the ERA-40 reanalysis. Observed P used in the VIC model (corrected for gauge catch deficiency) is compared with that from the ERA-40 reanalysis. Gridded values of evapotranspiration minus precipitation (E-P) are calculated from the ERA-40 atmospheric water budget, and estimates of implied E are obtained as the residual of observed P and ERA-40 E-P. The ERA-40 P is surprisingly close to observations on an annual basis over the large river basins (especially accounting for known errors in the observations). Furthermore, ERA-40 P is quite consistent with observations in terms of interannual, spatial, and latitudinal variations. ERA-40 E is generally higher than both VIC E and implied E in spring and autumn. However, VIC estimates more E in June and July than either ERA-40 or the atmospheric budget for the Yenisei, Ob, and Mackenzie River basins. The ERA-40 bias toward early snowmelt and a double runoff peak (not present in VIC or observations) indicates the need for improvements in the ECMWF land surface scheme. The long-term means of ERA-40 vapor convergence P-E for the Lena, Yenisei, Ob, and Mackenzie are not in balance with observed runoff, mainly due to the uncertainties in computed P-E and observed streamflow.

Citation: Su, F., J. C. Adam, K. E. Trenberth, and D. P. Lettenmaier (2006), Evaluation of surface water fluxes of the pan-Arctic land region with a land surface model and ERA-40 reanalysis, *J. Geophys. Res.*, *111*, D05110, doi:10.1029/2005JD006387.

1. Introduction

[2] The hydrologic cycle of the Arctic terrestrial drainage system is an important component of the global climate system. Runoff from northern flowing rivers represents approximately 50% of the net flux of freshwater to the Arctic Ocean, which is the only ocean with a contributing land area greater than its surface area [*Barry and Serreze*, 2000]. Terrestrial freshwater discharge to the Arctic Ocean plays an important role in determining the global thermohaline circulation, salinity, and sea ice dynamics [*Aagaard and Carmack*, 1989; *Macdonald*, 2000]. The freshwater budget of the Arctic has received attention also as a result of studies which suggest that global warming is expected to intensify the hydrologic cycle and the Arctic is a location of enhanced sensitivity to greenhouse gas emissions [*IPCC*, 1995]. A large body of evidence indicates that major climate-induced changes have already occurred, and many of these changes are linked to the Arctic hydrologic cycle [*Serreze et al.*, 2000; *Moritz et al.*, 2002; *Vorosmarty et al.*, 2001; *SEARCH SCC*, 2001]. These recent changes point to the need to better understand interactions among hydrologic cycle components.

[3] At present we have only a rough, qualitative understanding of the large-scale hydroclimatology of the Arctic. Better estimates are needed of the relative magnitudes of the terms in the Arctic terrestrial water budget, including precipitation (P), evapotranspiration (E), and runoff (R), and their spatiotemporal variability across major river basins and the entire pan-Arctic. In this paper we compare estimates of these water budget terms from observations, to the extent they are available, from an off-line run of the Variable Infiltration Capacity (VIC) macroscale hydrology model, and from the ERA-40 reanalysis [*Uppala et al.*, 2005].

[4] Reliable estimates of water budget components and other surface variables used to assess hydroclimatology variability and change are difficult to obtain from scattered measurements over large regions for long time periods, particularly in northern high latitudes. However, observations combined with models offer advantages for diagnoses of the freshwater budget of data sparse regions such as the Arctic. Land surface models capable of representing the dynamics of the land-atmosphere water and energy exchanges have been used in both off-line and coupled modes to simulate the water budget components in the pan-Arctic region [*Bowling et al.*, 2000; *Rawlins et al.*, 2003; *Arora*, 2001; *Walsh et al.*, 1998; *Kattsov et al.*, 2000; *Su et*

[1]Department of Civil and Environmental Engineering, University of Washington, Seattle, Washington, USA.
[2]National Center for Atmospheric Research, Boulder, Colorado, USA.

0148-0227/06/2005JD006387$09.00

al., 2005], and to evaluate the effects of climate change at scales ranging from large river basins to global [*Arora and Boer*, 2001; *Nijssen et al.*, 2001a]. Global reanalyses that incorporate all available (mostly atmospheric) observations in a model framework [e.g., *Kalnay et al.*, 1996; *Uppala et al.*, 2005], represent an additional data source for monitoring high latitude water budgets [*Cullather et al.*, 2000; *Rogers et al.*, 2001; *Betts and Viterbo*, 2000; *Betts et al.*, 2003a; *Serreze et al.*, 2003].

[5] *Bowling et al.* [2000] explored spatial and temporal variability of Arctic freshwater components based on observations, reanalysis convergence fields, and hydrologic model simulations. Their work suggested that (1) inconsistent and incomplete observed discharge data failed to provide a clear spatial pattern in runoff; (2) the convergence fields derived from the Goddard Earth Observing System (GEOS-1) data assimilation system were not good enough to depict E reasonably over the pan-Arctic domain, largely due to the relatively large (in absolute value) analysis increment present in GEOS-1 for the land surface water budget; and (3) the VIC macroscale hydrology model was able to provide continuous spatial and temporal representations of hydrologic variables in data scarce regions. Results from the climate model simulations of the Atmospheric Model Intercomparison Project (AMIP) [*Gates*, 1992] indicated that the AMIP models generally overestimate the Arctic precipitation P and precipitation minus evapotranspiration P-E, and P-E derived from the National Centers for Environmental Prediction/National Center for Atmospheric Research (NCEP/NCAR) reanalysis was closer to the observational estimates [*Trenberth and Guillemot*, 1998; *Walsh et al.*, 1998]. Walsh et al. suggested that the land surface parameterization should be an initial focus of diagnosis of water balance errors, given the close association between the variations of P and E in the AMIP models. *Serreze et al.* [2003] examined the large-scale hydroclimatology of the terrestrial Arctic drainage basin based on station data for precipitation and streamflow, and P-E derived from NCEP/NCAR reanalysis moisture flux convergence. For long-term water-year means, they found that calculated P-E for the Yenisey, Lena, and Mackenzie basins was 16–20% lower than observed runoff. They suggested that the new ERA-40 reanalysis might resolve the imbalance between atmospheric and surface water budgets.

[6] *Su et al.* [2005] reported off-line simulations of the VIC model implemented at 100 km EASE-Grid (Lambert azimuthal equal-area projection) across the pan-Arctic domain. In their work, pan-Arctic simulations, driven by the bias-corrected global precipitation data of *Adam and Lettenmaier* [2003] and *Adam et al.* [2006] were used to evaluate the model's representation of hydrologic processes in the Arctic land region. The model simulations of key hydrologic processes for the period of 1979 to 1999 were evaluated using observed streamflow, snow cover extent, dates of lake freeze-up and break-up, and permafrost active layer thickness. The VIC model was driven by gridded observed precipitation and temperature, and other forcings derived mostly from the daily temperature and temperature range (e.g., downward solar and longwave radiation; humidity) and closes the surface water balance by construct. The model estimates of regional-scale E are primarily based on the model's physics, whereas modeled runoff over the large areas represented by stream gauges was forced to match observations at least approximately via a process of parameter calibration. The calibration procedure is a trial and error process of estimating model parameters, such as soil depths and infiltration characteristics that are not well observed at large scales, so as to produce an acceptable match of model-predicted discharge with observations.

[7] When combining atmospheric and terrestrial water-balances, the water vapor convergence P-E should balance runoff R in the long-term annual average [*Oki et al.*, 1995; *Yeh et al.*, 1998; *Seneviratne et al.*, 2004]. One strategy for combining reanalysis water budget estimates with observations is to estimate the regional E as a residual from observed P and P-E [*Yeh et al.*, 1998; *Dai and Trenberth*, 2002; *Serreze et al.*, 2003].

[8] In the following section, the data sets and methodology used in this study are described. Subsequently, the surface water budgets from different estimates are compared explicitly for large Arctic river basins, for the entire pan-Arctic domain, and as a function of latitude.

[9] The overall motivation for this paper is to produce a better assessment of the water balance of the Arctic land area using two approaches: first, a calibrated off-line simulation with the macroscale VIC model, which is more or less forced to preserve observed runoff; and second, an atmospheric water budget based on the new ERA-40 reanalysis. Furthermore, various combinations of the two budgets with observations are used to diagnose differences and their causes. The results provide insights into how well the latitudinal, seasonal, and interannual variations of the surface hydrologic balance of the Arctic land region can be estimated using currently available data and methods. The evaluations also help identify surface processes that are poorly represented in the VIC and ECMWF land surface schemes.

2. Data and Methodology

[10] The VIC macroscale hydrology model [*Liang et al.*, 1994, 1996; *Cherkauer and Lettenmaier*, 1999, 2003] was used to simulate streamflow and other land surface hydrologic variables (evaporation, runoff, snow water storage) over the pan-Arctic land region at 100 km EASE-grid spatial resolution by *Su et al.* [2005]. In these simulations, the model was run in full energy balance mode (meaning that the model iterated for the effective land surface temperature so as to close both the surface energy and water budgets simultaneously). The model was forced with daily precipitation, maximum and minimum temperatures and wind speed for the period 1979 to 1999. Precipitation and temperature were from gridded observations, and wind speed from the NCEP/NCAR reanalysis. Vapor pressure, incoming shortwave radiation, and net longwave radiation were calculated based on daily temperature maxima and minima and precipitation using algorithms of *Kimball et al.* [1997], *Thornton and Running* [1999], and *Bras* [1990] which have been utilized in many earlier implementations of the VIC model [e.g., *Nijssen et al.*, 2001b; *Maurer et al.*, 2002]. Precipitation was adjusted for gauge undercatch and orographic effects, as described by *Adam and Lettenmaier* [2003] and *Adam et al.* [2006]. In particular, the effects of the *Adam et al.* [2006] orographic correction alone on mean

annual precipitation were increases of 20.64%, 21.65%, 3.29%, and 9.44% in the Lena, Yenisei, Ob, and Mackenzie, respectively. In this study, the precipitation used to drive the VIC model in the *Su et al.* [2005] pan-Arctic simulations, and the VIC-derived water budget variables (runoff and evapotranspiration) are compared with the same variables from the ERA-40 reanalysis to examine the seasonal and latitudinal water fluxes in the Arctic. Here we use a 21- year period (1979–1999) of VIC simulation and ERA-40 reanalysis.

[11] The ERA-40 reanalysis [*Uppala et al.*, 2005] is produced four times daily using the ECMWF numerical weather prediction (NWP) model, with a spatial resolution of approximately 125 km in the horizontal and 60 levels in the vertical. Model-derived fields are in most cases regridded and archived on a regular 2.5° latitude/longitude grid. The archived ERA-40 data including daily fields, monthly means, and monthly daily means are available from http://data.ecmwf.int/data/d/era40_daily/ on the standard 2.5° grid. Here we use 21 years of monthly daily means for the period 1979 to 1999. The ERA-40 archive includes surface fluxes of both water and energy variables derived entirely from the data assimilation model and thus are affected by deficiencies in model physics and parameterizations. Nonetheless, reanalysis products can provide valuable information about the land surface water and energy budgets for seasonal, interannual, and interbasin variability [*Betts and Ball*, 1999]. For this study, the 2.5° archived ERA-40 gridded data were interpolated to the 100 km × 100 km EASE grid across the pan-Arctic domain using an inverse distance interpolation. Higher resolution (about 1.41° latitude-longitude) ERA-40 surface reanalyses have become available http://www.cgd.ucar.edu/cas/catalog/ecmwf/era40) since the preparation of this paper. Given the relatively large areas over which we have performed the budgets we report, it is unlikely that the higher resolution data would result in substantial changes in our results.

[12] Monthly E-P (1958–2001) fields were computed at NCAR from ERA-40 wind, moisture, and surface pressure fields (which are strongly linked to observed data) using vertically-integrated moisture terms. This calculation was based on the raw ERA-40 data on a reduced T106 Gaussian grid with resolution about 1.13°. The E-P fields were subsequently interpolated to the 100 km EASE grid.

[13] The atmospheric water budget can be estimated as follows:

$$\frac{\partial Wa}{\partial t} + \nabla.Q = E - P \tag{1}$$

$$Wa = \frac{1}{g}\int_0^{p_s} q dp \tag{2}$$

$$Q = \frac{1}{g}\int_0^{p_s} q\vec{V} dp \tag{3}$$

where $\nabla.Q$ is the horizontal divergence of vertically integrated atmospheric vapor flux, Wa is the precipitable water (or total column water vapor in the atmosphere), q is specific humidity, $\vec{V}$ is the horizontal wind velocity, p is pressure, and p_s is the surface pressure. Liquid and solid water in clouds and their horizontal transports are ignored in equation (1) as they are small compared with the water vapor amount [*Trenberth and Smith*, 2005]. The two terms on the left-hand side of equation (1) can be computed from the ERA-40 reanalyses to produce a field of E-P. For this study, we computed the atmospheric water budget using methods outlined by *Trenberth and Guillemot* [1995] and *Trenberth* [1997]. We combined E-P with the gridded observed P used in the VIC model to compute implied E, in addition to value of E produced directly by the VIC model, and by the ERA-40 reanalysis. A similar strategy was applied globally by *Dai and Trenberth* [2002].

[14] The land surface water balance is expressed as:

$$\frac{\partial Ws}{\partial t} = P - E - R \tag{4}$$

where Ws represents the soil water storage and R is the total runoff. By averaging (1) and (4) over long time series, the changes of the annual mean atmospheric vapor and soil water can be neglected. Thus we derive the following equation when combining (1) and (4) for multi-year averages:

$$\overline{R} = -\nabla.\overline{Q} = \overline{P} - \overline{E} \tag{5}$$

which is an expression of the fact that over long periods, the horizontal flow of water vapor into a land region by atmospheric transport is balanced by the river and subsurface flow out of the region. The approach of relating surface water fluxes to the atmospheric moisture budget has been used to study terrestrial water storage and regional E estimates by others [*Roads et al.*, 1994; *Oki et al.*, 1995; *Yeh et al.*, 1998; *Dai and Trenberth*, 2002; *Seneviratne et al.*, 2004]. In this study, we examine the agreement between the long-term means of P-E from the atmospheric moisture budget and the runoff (R) from a surface water balance in the Arctic land area. Our basic methodology is to compare the land surface water fluxes from a 21-year off-line simulation of the VIC model in the Arctic land area with the same variables represented by the land surface scheme in ERA-40, and to examine the E simulations from the VIC and ERA-40 model with the residual estimates from moisture convergence (P-E) and observed P. We examine the seasonal variability of P, E, and R both for the largest Arctic river basins, and for the entire pan-Arctic domain. Furthermore, we examine the moisture flux trends with latitude in Eurasia and North America. Here P-E is the exact opposite to E-P, and in this paper we use the two interchangeably. Figure 1 summarizes the data sources used in this study.

3. Results

3.1. Basin-Wide Comparisons

[15] The Lena, Yenisei and Ob rivers are the three largest Eurasian rivers flowing into the Arctic Ocean, with drainage areas ranging from 2.4×10^6 to 3.0×10^6 km^2. The Mackenzie basin, with a drainage area of 1.8×10^6 km^2,

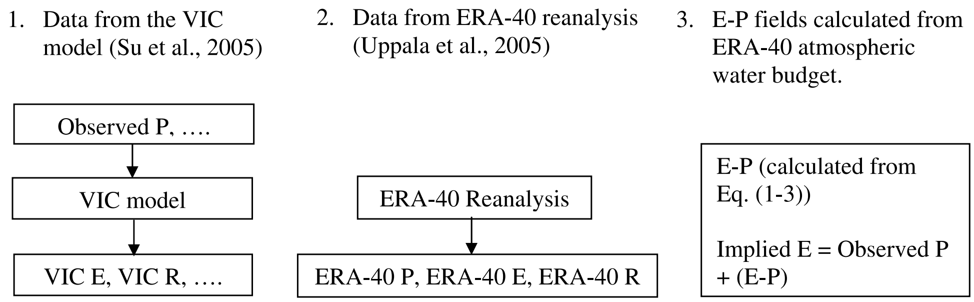

Figure 1. Diagram of different data sources used in this study.

is the largest North American river basin (Figure 2). These four rivers account for about 68% of the total river discharge into the Arctic Ocean [*Grabs et al.*, 2000]. To assess the interannual and seasonal variability of the water balance components in different data sets at a basin-wide scale, the monthly time series and seasonal means of each component are spatially integrated over the Lena, Yenisei, Ob and Mackenzie (Figures 3–6). Two sets of precipitation and runoff (observed P and ERA-40 P, VIC R and ERA-40 R), and three evapotranspiration products (VIC E, ERA-40 E, and Implied E) are shown in Figures 3–6.

[16] The Arctic freshwater budget and land surface hydrologic system is driven primarily by precipitation. The ERA-40 P is quite similar to the observed P in terms of interannual variations for all four basins (left-hand side of Figures 3–6a). The variance explained r^2 (where r is the correlation coefficient) for regressions of the 21-year time series of monthly observed P on ERA-40 P are 0.87, 0.85, 0.89, and 0.86 for the Lena, Yenisei, Ob, and Mackenzie respectively, suggesting considerable veracity of the ERA-40 P in the Arctic area. Figures 3–6a (right-hand side) compare the basin-wide average mean monthly P for ERA-40 and observations. P is lowest in February and March and highest during July for all four basins. The seasonality of precipitation is well represented by ERA-40. However, the ERA-40 P tends to be too low during the summer for the Lena and Yenisei, during May to October for the Ob, and during August to February for the Mackenzie. The annual average ERA-40 P (1979–1999) is less than the estimate from observations by about 6% for each of these four basins

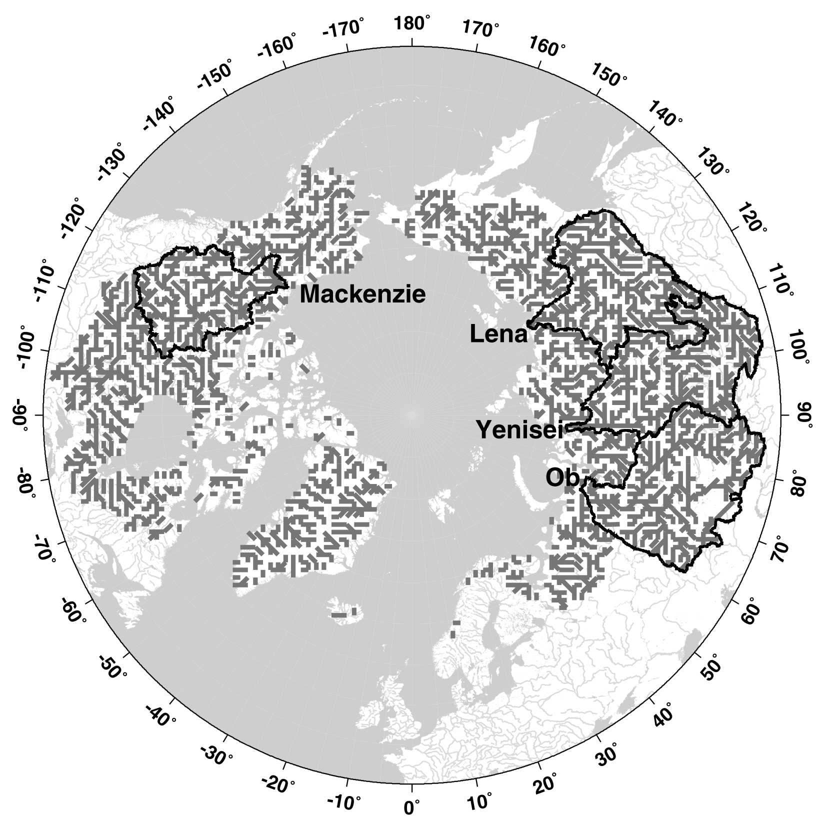

Figure 2. Digital river networks for the pan-Arctic drainage basins at the 100 km resolution, showing the watershed boundaries of the Lena, Yenisei, Ob, and Mackenzie.

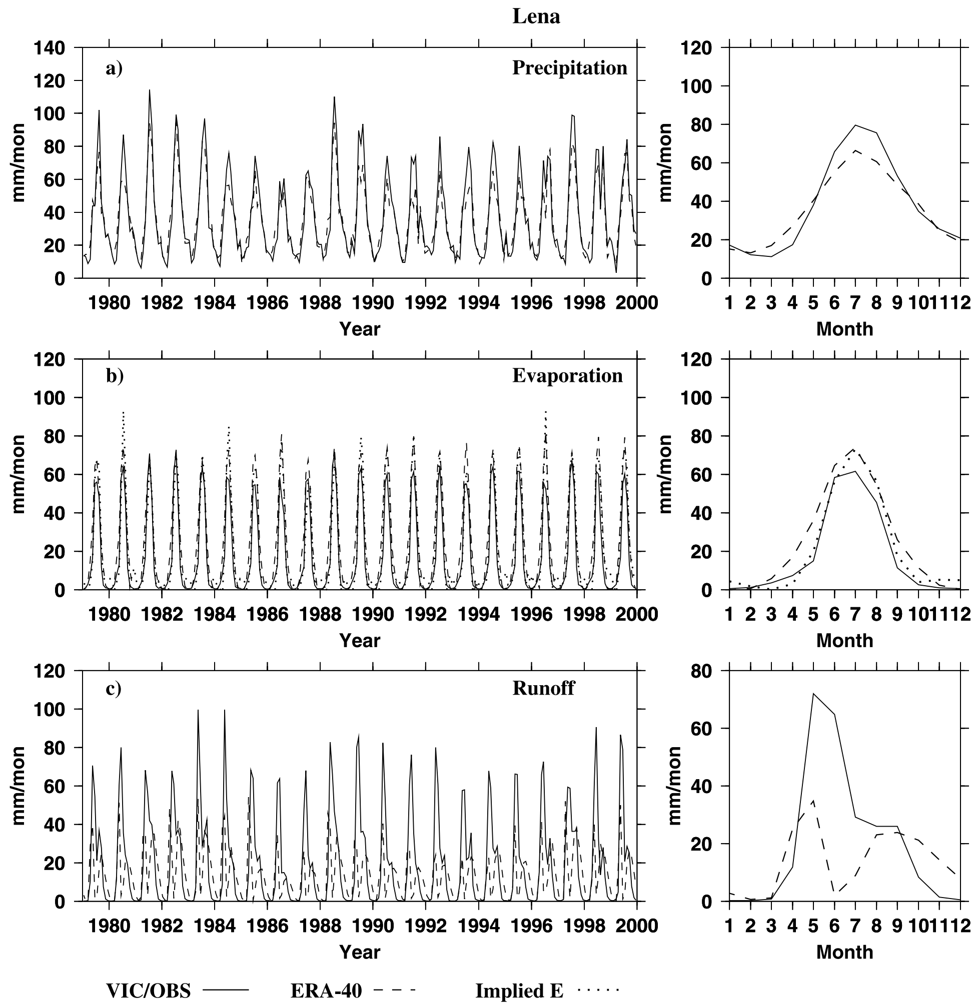

Figure 3. Monthly time series (left-hand) and seasonal means (right-hand) of water budget components from the VIC model (solid), ERA-40 reanalysis (dashed), and implied E (dotted) for the Lena basin: (a) precipitation (P); (b) evapotranspiration (E); (c) runoff (R). Observed precipitation used in the VIC model in Figure 3a is also shown as solid lines. All the units are in mm/month.

(Table 1). This difference is surprisingly small given uncertainties in precipitation due to sparse station coverage, the effects of gauge catch corrections, and of orographic corrections. In fact, the effects of the above two adjustments, which are present in the data we used based on recent work by *Adam and Lettenmaier* [2003] and *Adam et al.* [2006] are considerably larger than the 6 percent difference between VIC and ERA-40 P. We note that the *Su et al.* [2005] VIC simulations of streamflow overestimate observations in the Lena and Yenisei somewhat, and these are coincidentally the basins with the largest precipitation adjustments. In any event, the ERA-40 P seems to well represent annual amounts and monthly variations over the four largest Arctic basins, despite the differences in long-term seasonal means (possible underestimation in most cases), consistent with *Serreze et al.* [2005] and *Betts et al.* [2003a].

[17] Figures 3–6b show the monthly time series and mean seasonal cycle of evapotranspiration (E) estimates from the VIC model, ERA-40 reanalysis, and atmospheric budget (Implied E). E has similar seasonal variations among the three estimates, which are low during October to April and peak in July. The ERA-40 E is consistently higher than the VIC and atmospheric budget estimates from September through May in all basins. Annual E from ERA-40 is higher than the VIC estimates by 40%, 16%, 16%, and 29% for the Lena, Yenisei, Ob, and Mackenzie basins respectively (Table 1).

[18] E from the VIC model and atmospheric budget agree more closely during the spring and autumn than with the ERA-40 reanalysis. The winter season (October through February) E in VIC is extremely low (<3 mm) for the four basins, and is much less than the atmospheric estimates. However, the VIC model estimates more E in June and July than both the ERA-40 and atmospheric budgets for all the basins with the exception of the Lena. The annual E from the atmospheric budget and estimated P is higher than the VIC estimates by 18%, 4%, 6%, and 15% for the Lena, Yenisei, Ob, and Mackenzie respectively (Table 1). The variation of implied E in winter months is fairly consistent with that of observed P (e.g., Figure 6b) which suggests that the moisture convergence E-P plays less of a role than do differences in P.

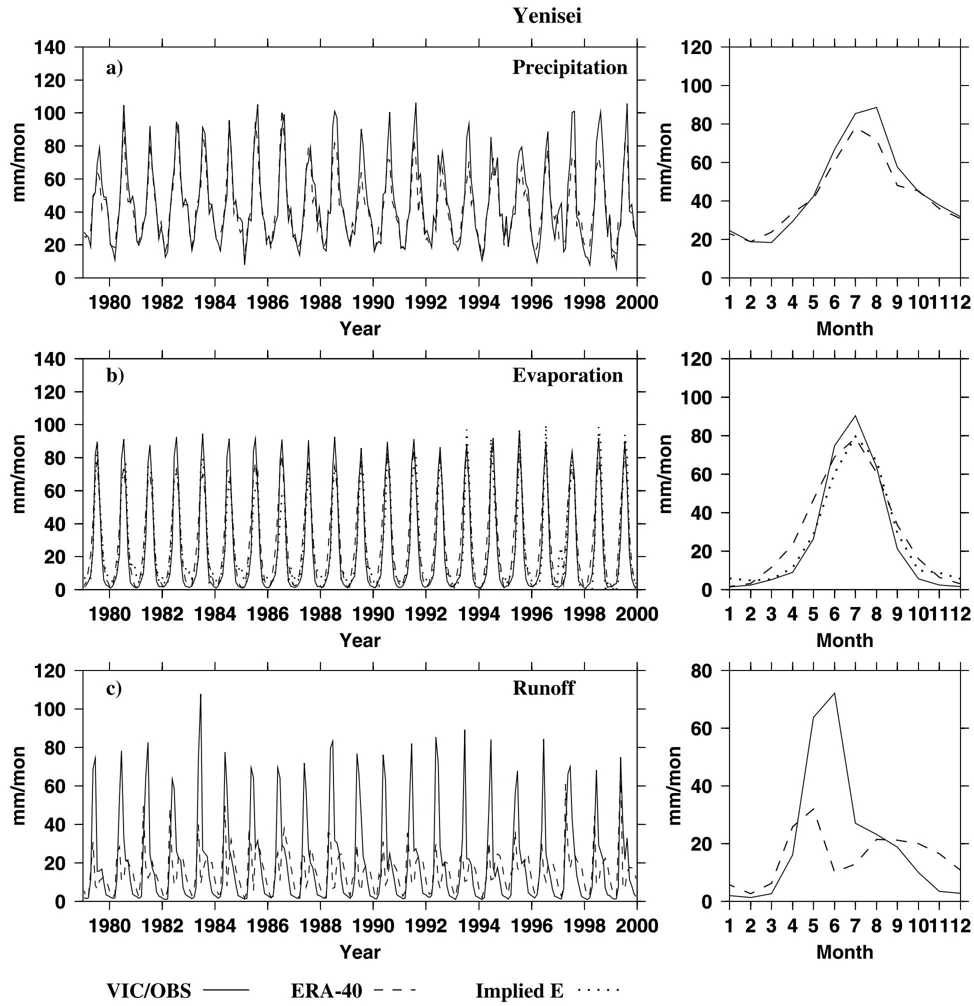

Figure 4. Same as Figure 3, but for the Yenisei basin.

[19] Monthly time series of runoff (unrouted) and seasonal means from the VIC and ERA-40 reanalysis (Figures 3–6c) differ considerably. Streamflow simulations in *Su et al.* [2005] were close to observations for the four largest Arctic basins (with annual average biases less than13% and generally good representations of the observed seasonal cycle). The VIC runoff is low from November to April and has a sharp peak in May arising from snowmelt, and gradually declines from August through April. The rainfall-runoff in summer is much lower than the spring snowmelt flood. In contrast, the snowmelt floods in the ERA-40 occur one month earlier in April, and there is a large second peak in August for the Lena and Yenisei. A smaller second runoff peak in the ERA-40 occurs in August for the Mackenzie, while it occurs in November for the Ob.

[20] Table 1 lists annual mean values of P, E, and R from different datasets, and nonclosure terms in VIC and ERA-40 (also see Figure 7). In the case of VIC, nonclosure results (generally small) from changes in subsurface and snow storage over the period of simulation. In ERA-40, storage change is generally a minor source of nonclosure; the larger source is the analysis increment (due to soil moisture nudging and snow depth assimilation). The surface water imbalance in ERA-40 is between −29 and −119 mm, which accounts for 6%–27% of annual P for the four Arctic basins. The Ob (−62 mm) and the Mackenzie (−119 mm) show the biggest imbalances, most of which comes from the snow water increments in these two basins (Table 2, −56 mm for the Ob, and −88 mm for the Mackenzie). The surface water imbalance (−119 mm) in the Mackenzie is close to the total analysis increment (114 mm) found in *Betts et al.* [2003a].

[21] All the moisture terms are calculated for the gauged part of each basin, which covers more than 90% of the entire basin. Also, by expressing the surface fluxes and storage terms as depths averaged over the area, the effect of mismatches in drainage areas is minimized. According to equation (5), aside from estimation errors the long-term means of vapor convergence P-E should be equal to R. From Table 1, convergence P-E and observed R agree within 9%, with a P-E deficit of 8.1%, 6.1%, 8.4%, and 8.5% for the Lena, Yenisei, Ob, and Mackenzie, respectively.

3.2. Spatial Fields

[22] Figure 8 shows the spatial distribution of seasonal averages of precipitation from the gridded observations and ERA-40, and the difference between the two for winter

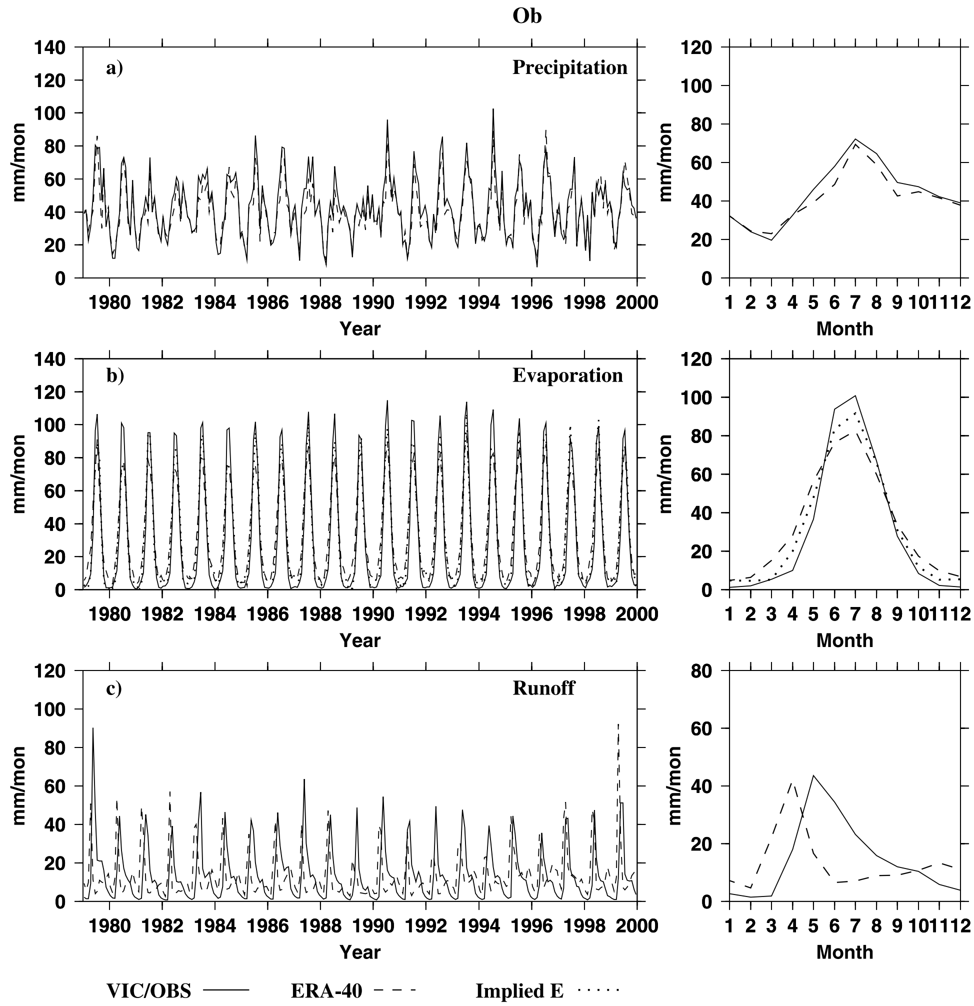

Figure 5. Same as Figure 3, but for the Ob basin.

(DJF), spring (MAM), summer (JJA), and autumn (SON). The ERA-40 values agree reasonably well with the observations both in the timing and magnitude of the seasonal pattern of P. Winter and spring P is low over much of eastern Eurasia, northern Alaska and Canada, and the Canadian Archipelago. P peaks in summer over most land areas, and is persistently high over Hudson Bay, Barents and coastal Norway, and parts of the Yenisei and Ob basins in autumn. Extremely high P is seen along the south of Alaska, southeast Greenland, and Norwegian coast in almost all seasons. Although the distribution of seasonal P is consistent between ERA-40 and observations, significant differences are evident in some areas. ERA-40 tends to underestimate P in comparison with observations over most land areas, particularly over southern Alaska, southeastern Greenland, and the Norwegian coast, where both ERA-40 and observations exhibit P maxima. Along the Arctic coast, ERA-40 overpredicts P in the summer and autumn for North America, and in all seasons for Eurasia.

[23] The spatial distribution of seasonal average evapotranspiration from VIC and ERA-40, and implied E are shown in Figure 9. In winter, E from VIC is essentially zero for almost all the land areas, and is generally less than 20 mm in spring over southern Eurasia and North America. The implied E and ERA-40 E are also small in cold seasons, but are generally higher than the VIC estimates. High values (40–100 mm) in cold seasons in the implied E and ERA-40 E are observed along the very southern part of Alaska, southeastern Greenland, and Norwegian coast, corresponding to the highest precipitation (Figure 8) and winter surface temperatures. The high precipitation and temperature alone do not explain the high winter E in ERA-40, since VIC has the same distribution of precipitation and temperature, but much lower E in the same areas. The differences are most likely due to the analysis increments in ERA-40, and different physical representations of E in the ERA-40 and VIC land surface schemes. The high bias in ERA-40 E has also been found in some other studies [*Betts et al.*, 2003a, 2003b], however we cannot be sure that the small VIC E in winter is correct. Implied E is calculated as a residual of observed P and ERA-40 convergence. The winter implied E is much higher (60–120 mm) than both the VIC and ERA-40 in most land areas with the highest observed P. All the data sets show maxima in E in summer coincident with the maximum temperatures (not shown). E decreases poleward in both Eurasia and North America, in

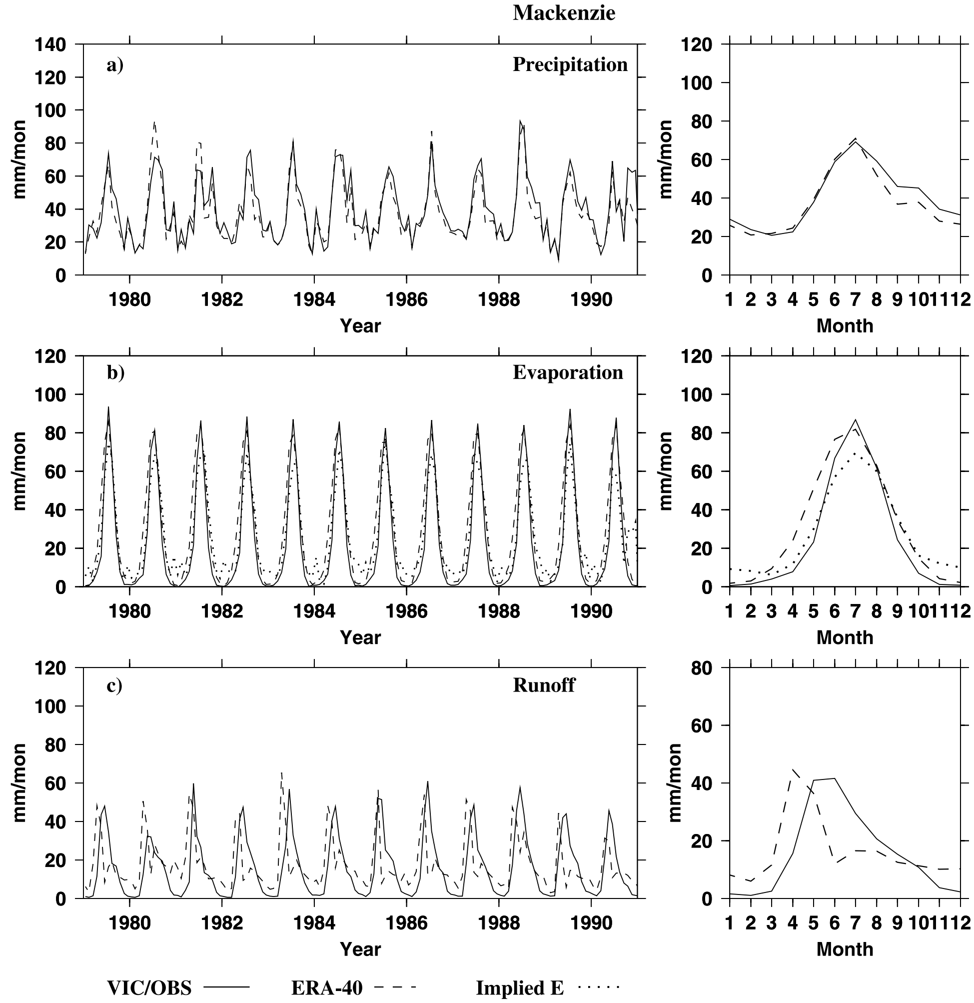

Figure 6. Same as Figure 3, but for the Mackenzie basin.

concert with zonal changes in surface temperature. The implied E is slightly negative over parts of Eurasia, the Canadian Archipelago, and western Greenland through all the seasons. In general, E from the VIC and ERA-40 model, and atmospheric budget show similar seasonal and spatial variations for most of the Arctic land areas, although large difference exists in absolute values.

[24] Runoff in the VIC model is relatively low over much of the terrestrial Arctic in cold season due to the lack of groundwater contribution in the model. Compared with observations, the VIC model considerably underestimates baseflow in the cold season by 49%–78% for the major Arctic basins [*Su et al.*, 2005]. In most cases the peak values, mainly caused by snowmelt, occur during the period of May to June, and are reproduced well by VIC. Runoff in ERA-40 (not shown) begins to increase in the southernmost part of the domain in both Eurasia and North America in March, and propagates northward in both magnitude and extent in April, with peaks during April to May. In general, the ERA-40 peak runoff is about one month earlier than in the VIC model, which matches observations quite closely, as shown by *Su et al.* [2005].

Table 1. Annual Average Precipitation (P), Evapotranspiration (E), and Runoff (R) From the Observations (OBS), VIC Model, and ERA-40 Reanalysis for the Lena, Yenisei, Ob, and Mackenzie From 1979 Through 1999, and Nonclosure Terms in VIC and ERA-40

	P, mm		E, mm			R, mm				P-E-R	
	OBS	ERA-40	VIC	ERA-40	Implied[a]	VIC	ERA-40	P-E[b]	OBS	VIC	ERA-40
Lena	452	426	209	293	247	242	166	204	222	1	−33
Yenisei	546	511	304	354	317	243	185	229	244	−1	−29
Ob	527	495	356	397	377	173	160	151	165	−2	−62
Mackenzie	477	444	285	367	327	185	196	150	164	7	−119

[a]Implied E = observed P + (E-P).
[b]P-E = −(E-P).

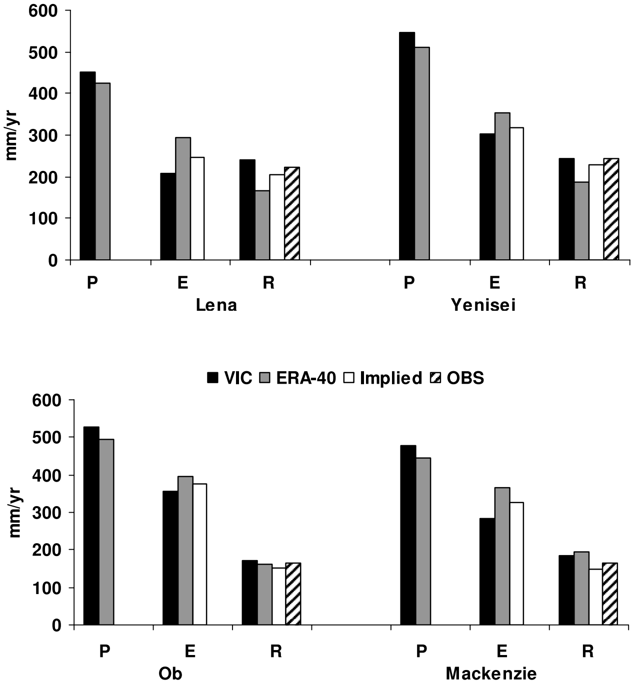

Figure 7. Mean annual precipitation (P, mm), evapotranspiration (E, mm), and runoff (R, mm) from different data sets for the Lena, Yenisei, Ob, and Mackenzie (corresponding to Table 1). The observed R (OBS) was normalized by the gauged area reported by R-ArcticNet.

[25] Although multi-annual mean P-E calculated from the atmospheric water balance should balance runoff, there are considerable differences. Fields of VIC simulated annual mean R, annual vapor convergence P-E, and annual ERA-40 R are shown in Figure 10. There is generally a good correspondence between the annual P-E and VIC R in spatial variations (Figures 10a and 10b). Nonetheless, the correlation coefficient (r = 0.65) between the P-E and VIC R across all the [2834] grid cells is modest. Some negative values of P-E appear mainly over the low-runoff regions, such as the southwestern Ob and Nelson where irrigation may distort the budgets. The annual R over the southern Yenisei is relatively low (50–100 mm) in VIC, while P-E exhibits much higher values (300–400 mm) in the same region (corresponding to the negative implied E in Figure 9), which are obviously wrong in the determination of E-P. Reliable long-term P-E from reanalysis atmospheric water balance provides another potential way to study decadal trends of continental discharge and river inflow to the world oceans [*Dai and Trenberth*, 2002]. Annual R in ERA-40 (Figure 10c) is near zero along the central coast, and some of southern Alaska and coastal Norway where the VIC and P-E exhibit maxima. The interpolation from 2.5° ERA-40 fields to 100 km EASE grid may produce some errors along the central coast, while the problems in southern Alaska and coastal Norway are probably due to the extremely high annual E in ERA-40 (not shown). Except for the coastal areas, the ERA-40 annual R shows roughly consistent distributions with the VIC R and P-E fields.

3.3. Latitudinal Trends

[26] Figures 11 and 12 show the annual means of P, E, and R versus latitude for North America and Eurasia from observations, VIC, ERA-40, and atmospheric water budget. P in both observations and ERA-40 is maximum (700–900 mm) in the 55–60°N band for North America (Figure 11a) (due in large part to effects of high P in southern Alaska), then decreases sharply with latitude. P for North America from 65–80°N comes mainly from the north of Alaska, the Canadian Archipelago, and the northern Hudson Bay region, where P tends to be low (200–400 mm). ERA-40 P and observations have quite similar latitudinal changes for North America. However, ERA-40 P is generally less than observations, especially for 45–65°N, which covers most of the North American land area.

[27] For Eurasia (Figure 12a), P in ERA-40 increases with latitude up to 55–60°N above which it begins to decrease gradually. The observations show a similar pattern, with observed P peaking in the 60–65°N band, mainly due to high values along the Norwegian coast, and north central Eurasia. In general, the latitudinal patterns of P from ERA-40 and observations are consistent.

[28] E over North America (Figure 11b) for the southernmost latitude band (45–50°N) is around 500 mm for all three estimates. The values decrease poleward to about 50–100 mm in the highest latitude band (75–80°N), consistent with the changes of annual radiation and temperature (not shown). However, the estimates generally become less consistent (at least in a relative sense) with latitude. E in ERA-40 is higher than from VIC by 15–63% in the zones 50–70°N. Implied E is higher than both VIC and ERA-40 for all latitudinal bands in North America.

[29] In Eurasia (Figure 12b), VIC and ERA-40 also show similar latitudinal patterns of E, with E decreasing gradually from 50–55°N northward. However, ERA-40 E is always higher than VIC. Implied E seems surprisingly low in 45–50°N (205 mm), although this band is close to the semi-arid and arid regions of central Asia and slight displacement of the general circulation could account for this behavior.

[30] For North America, VIC R and P-E increase with latitude up to 55–60°N corresponding to the peak precip-

Table 2. Annual Mean Snowfall (SF), Snowmelt (SM), Snow Evaporation (SE), and the Imbalance (SF-SM-SE) in the ERA-40 Reanalysis for the Lena, Yenisei, Ob, and Mackenzie (1979–1999)

	Snowfall, mm	Snowmelt, mm	Snow Evaporation, mm	Imbalance, mm	SE/SM, %
Lena	159	123	42	−6	34
Yenisei	190	140	53	−3	38
Ob	154	155	55	−56	35
Mackenzie	146	195	39	−88	20

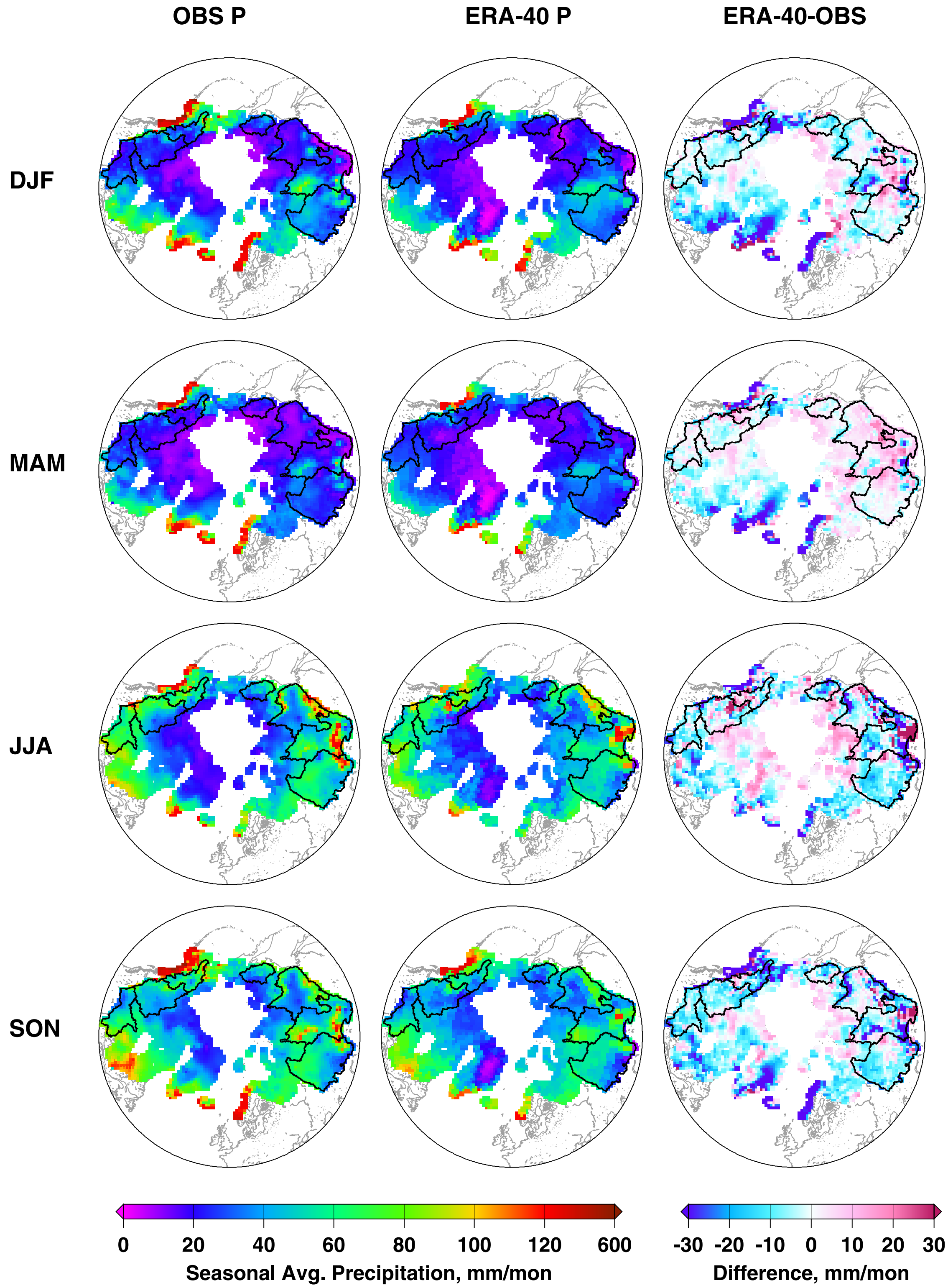

Figure 8. Spatial distribution of seasonal average precipitation (mm/month) from the gridded observations (OBS) and ERA-40 reanalysis, and the difference between the two fields for the Arctic drainage basin (1979–1999).

itation in this band (Figure 11a), and then they begin to decrease. ERA-40 R does not show such a clear pattern as the other two estimates, and considerably underestimates R in latitudes 55–65°N. VIC R is higher than the P-E in all latitudes for North America. These results contrast with the runoff patterns inferred for both hemispheres by *Bowling et al.* [2000], although we suspect that the differences are primarily due to difficulties in assigning limited gauged

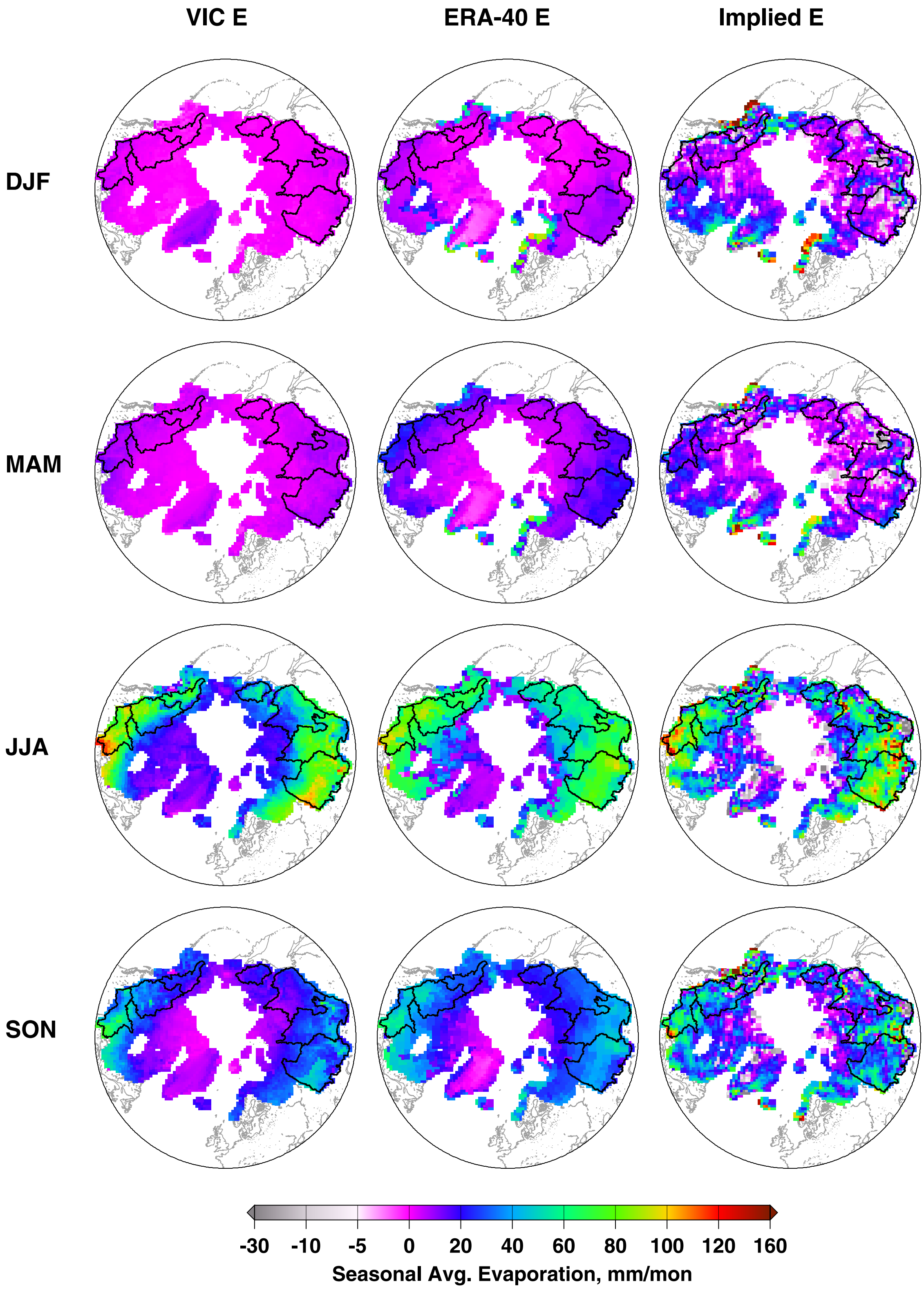

Figure 9. Spatial distribution of seasonal average evapotranspiration (mm/month) from the VIC and ERA-40 simulations, and atmospheric water budget estimates (implied E) for the Arctic drainage basin (1979–1999).

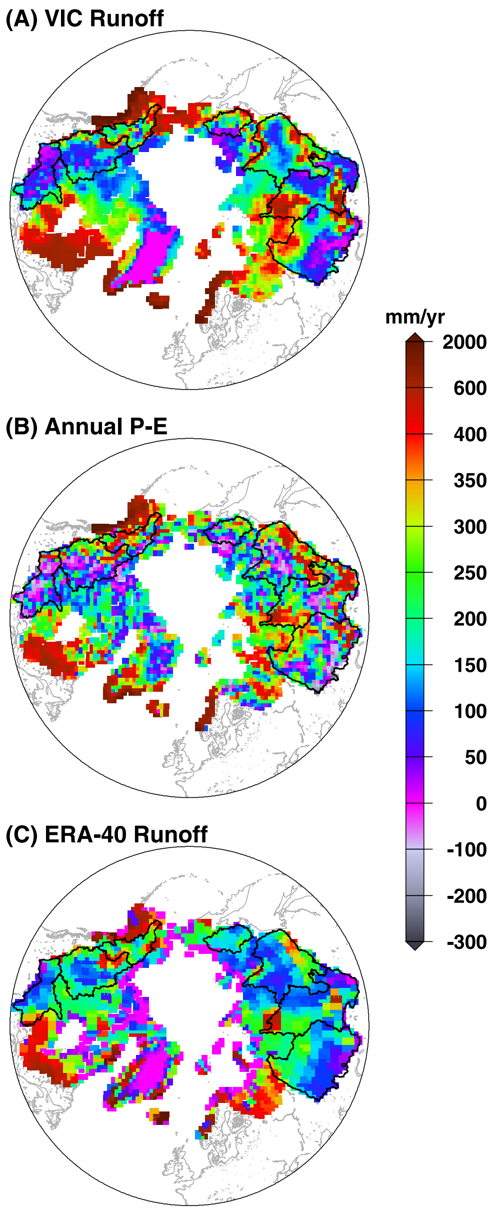

Figure 10. Fields of (a) VIC simulated annual mean runoff (mm) (1979–1999), (b) annual mean moisture convergence P-E (mm), and (c) annual mean ERA-40 runoff (mm).

discharge data to latitude bins in *Bowling et al.* [2000]. Significant differences exist among the estimates of R for Eurasia (Figure 12c). The VIC runoff distribution with latitude is consistent with the latitudinal changes of observed P, with peaks occurring for 60–70°N (Figure 12a), indicating the control of precipitation on runoff spatial variability. Similar changes are observed in P-E (except for 45–50°N), and ERA-40 R; however, both these estimates are less than VIC for most latitude bands.

[31] We also investigate three estimates (VIC R, ERA-40 R, and P-E) of the fraction of annual total discharge into the Arctic Ocean for each 5° latitude zone from Eurasia and North America (figures not shown). Flows into the Hudson Bay, Yukon, and Greenland are not included in this calculation. Our analysis shows that runoff originating between 60°–70°N accounts for 40% of Eurasian discharge from the VIC R and ERA-40 R, and about 30% from the atmospheric convergence P-E. This area covers the Barents, Kolyma, and most of the largest Siberia basins. The atmospheric convergence estimate of discharge originating at low latitude (45–50°N) is much higher (21%) than either VIC (7%) or ERA-40 (8.6%). For North America, runoff originating from 50–65°N accounts for about 70% of the total discharge from the VIC and implied P-E (60% from the ERA-40 R). In North America, runoff originating at the highest latitudes (65–80°N, most of which is located in the northern Mackenzie and Canadian Archipelago) accounts for about 30% of North American discharge by all three estimates.

4. Discussion

[32] In the work of *Su et al.* [2005], the VIC model was calibrated over the entire pan-Arctic drainage basin by

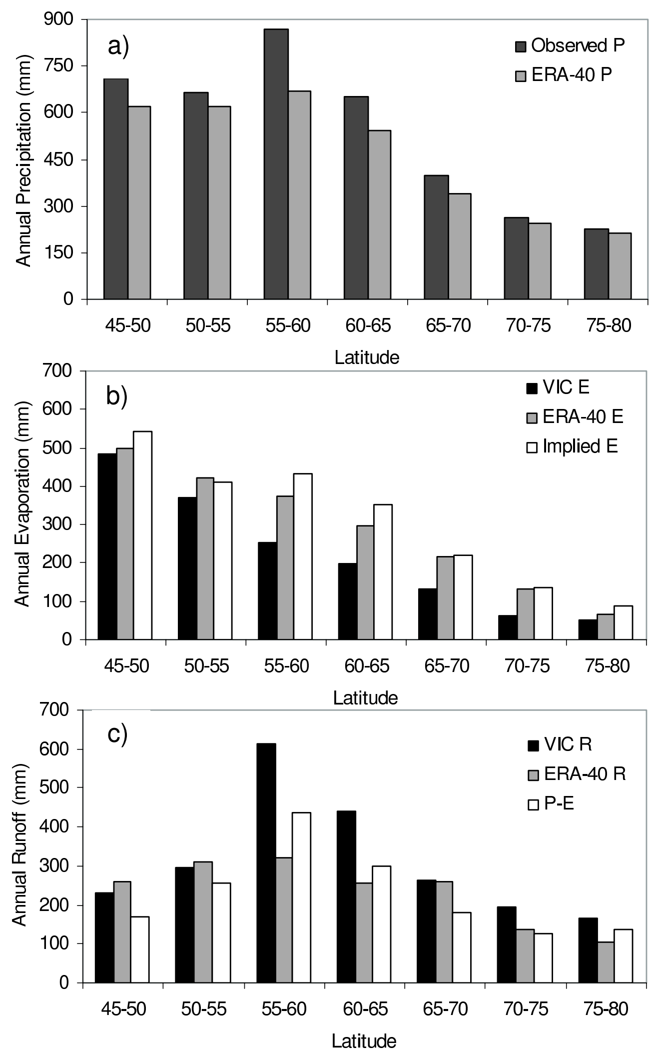

Figure 11. (a) Annual mean precipitation (mm), (b) evapotranspiration (mm), and (c) runoff (mm) versus latitude for North America from the observations, VIC model, ERA-40 reanalysis, and atmospheric water budget (implied E or P-E).

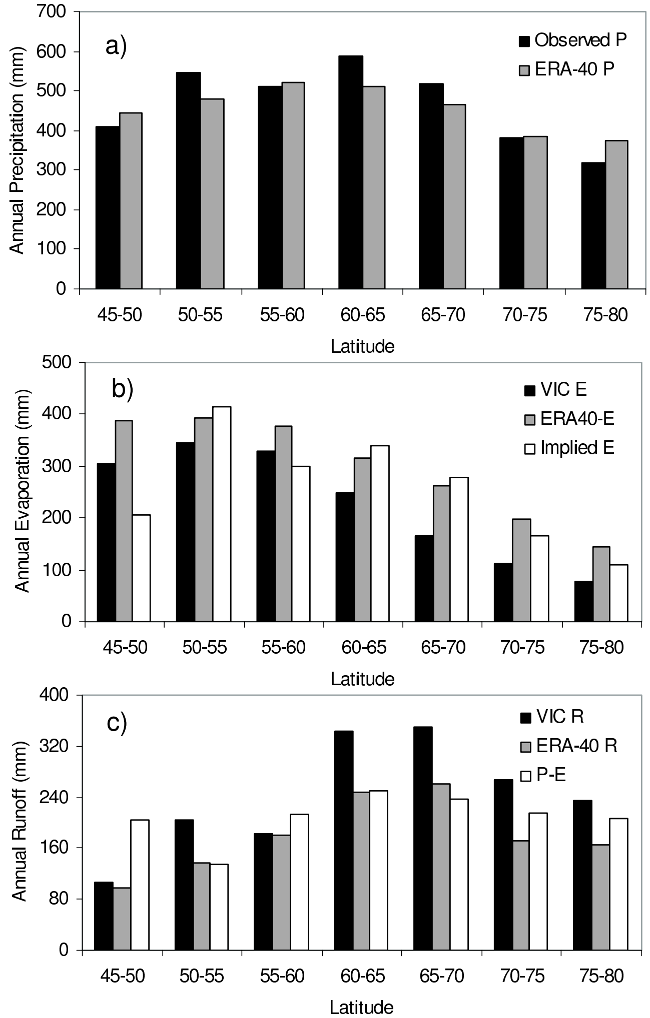

Figure 12. (a) Annual mean precipitation (mm), (b) evapotranspiration (mm), and (c) runoff (mm) versus latitude for Eurasia from the observations, VIC model, ERA-40 reanalysis, and atmospheric water budget (implied E or P-E).

matching the shape of observed monthly hydrograph and the volume of annual mean runoff. The results suggested that the model was able to reproduce the observed streamflow and some other hydrologic processes reasonably well, but also revealed that the model is highly sensitive to the precipitation forcings, which are subject to considerable observation errors. Also, human activities, such as fragmentation of the river channels by dams, inter-basin diversion, and irrigation, are not accounted for in the observed streamflow data which were used for calibration. Although these effects are expected to be modest for the largest Arctic river basins, the effects of both precipitation estimation errors and human influences on streamflow nonetheless add uncertainties to the estimation of evapotranspiration by the land surface model.

[33] The apparent over simulation of E in summer by the VIC model may be due in part to errors in estimates of observed P. The VIC model was driven by observed precipitation and validated against observed streamflow. If both precipitation and streamflow are correct, over a long period (generally multiple decades), evaporation should be realistically estimated by the VIC model [*Maurer et al.*, 2002]. Similarly, previous studies [e.g., *Ropelewski and Yarosh*, 1998; *Yeh et al.*, 1998] suggest that residual estimates from moisture convergence and observed precipitation should provide accurate estimates of the climatology of E over relatively large areas, subject to certain issues in estimation of the convergence. Comparable and consistent estimates of regional E from both an atmospheric budget and the VIC model were found in earlier implementations of the VIC model over the Arkansas-Red [*Abdulla et al.*, 1996] and Mississippi River basins [*Maurer et al.*, 2001]. However, because uncertainties in both observed P and P-E influence the VIC and residual estimates, respectively, we cannot conclude which estimate of E is most credible, at least not absent other information.

[34] *Betts et al.* [2003a] estimated a similar high bias (30%) of annual E from ERA-40 for the Mackenzie. *Betts et al.* [2003b] also found an upward bias in E in the spring and fall in ERA-40 for the Mississippi basin, and suggested that one possible reason was the lack of a realistic seasonal cycle in the vegetation model used in ERA-40 (fixed Leaf Area Index). Furthermore, the analysis increments play an important role in the ERA-40 model hydrology [*Betts et al.*, 2003a].

[35] Because evaporation in the model is strongly coupled to soil water, we suspect that the soil water nudging is at least partly responsible for the high biases in the ERA-40 E. Previous studies [e.g., *Betts et al.*, 2003a, 2003b] have not isolated the cause of apparent over estimation of E in the ERA-40 reanalysis. Off-line evaluation of the ECMWF land scheme used in ERA-40 showed a significant improvement of simulated E for a boreal (BOREAS) relative to an earlier version of the ECMWF land surface scheme [*Van den Hurk et al.*, 2000], although some upward bias in high latitude E persisted in the version of the land scheme used in ERA-40. Based on our results, we cannot definitively isolate a cause for the apparent upward bias, although we suspect that it may be largely due to the structure of the land scheme.

[36] The double runoff peaks and early snowmelt in ERA-40 runoff (Figures 3–6c) have been found and discussed in other studies [*Betts et al.*, 2003a; *Van den Hurk et al.*, 2000]. The first peak comes from snowmelt, which occurs quickly once sufficient melt energy is available in spring. This fast response is accentuated by frozen ground. The second peak (in the ERA-40 model) comes from subsurface drainage which is trapped on top of lower frozen layers. This water is released only when the lowest model layer melts and reaches a soil moisture threshold. The early melt in the ERA-40 land surface model is still under investigation. *Betts et al.* [2003a] suggest that it may be related to simplification in the snow thermal budget and a warm temperature bias in April. *Van den Hurk and Viterbo* [2003] report improvements to the ECMWF land surface scheme in both the timing and amount of runoff in cold regions, but these improvements were not incorporated in the version of the land surface scheme used in ERA-40.

[37] In PILPS 2(e) (Project for Intercomparison of Land Surface Parameterization Schemes) the ECMWF land surface scheme greatly overestimated sublimation, and underestimated spring snow accumulation, and hence snowmelt runoff [*Bowling et al.*, 2003]. A check of the frozen water

budget in ERA-40 (snowfall, snowmelt, and snow evaporation) (Table 2) showed that the snow E accounts for 20%–38% of the accumulated (over the winter period) snowpack for the Lena, Yenisei, Ob, and Mackenzie basins, or generally less than half the spring melt. This much smaller sublimation suggests a significant improvement in the ERA-40 frozen moisture budget relative to PILPS 2(e) and some early studies [*Betts and Ball*, 1999; *Betts and Viterbo*, 2000].

[38] The biases between ERA-40 atmospheric convergence P-E and observed R (less than 9% in absolute value) for the four largest Arctic river basins (Table 1) are smaller than those found by *Serreze et al.* [2003] (9–20%) when using the NCEP/NCAR reanalysis. Imbalances between P-E and runoff have also been found in several other studies investigating atmospheric water balances with reanalysis [*Roads et al.*, 1994; *Oki et al.*, 1995; *Gutowski et al.*, 1997; *Yeh et al.*, 1998; *Seneviratne et al.*, 2004]. These biases are postulated to be due chiefly to inaccuracies in the atmospheric water vapor convergence calculated from the analysis system, as long-term streamflow average are thought to be accurate to within a few percent [*Gutowski et al.*, 1997; *Seneviratne et al.*, 2004].

[39] Negative implied E is also present in NCEP/NCAR and ERA-15 reanalyses, despite the use of different observed precipitation [*Serreze et al.*, 2003; *Dai and Trenberth*, 2002]. While it is physically possible to have negative E over land (e.g., condensation), particularly in winter, it appears much more likely that the negative implied E in Figure 9 arises from underestimation of E-P. The much higher value of P-E (or lower value of E-P, Figure 12c) and lower value of implied E (Figure 12b) for the latitudes of 45–50°N in Eurasia may indicate errors in the calculation of E-P in this band. Our ongoing study indicates that problems with ECMWF E-P in lower latitudes are greater and negative P-E in Figure 10b are in general errors.

[40] The use of P-E and implied E calculated from the reanalysis atmospheric moisture budget is a powerful tool for quantifying the continental water cycle and for verifying macroscale hydrologic models [*Oki et al.*, 1995; *Yeh et al.*, 1998; *Maurer et al.*, 2001]. Results reported here indicate that the annual evapotranspiration from the VIC model is generally lower than the implied E, while the VIC annual runoff is mostly higher than the P-E for both hemispheres (Figures 11c and 12c), although the two estimates show somewhat consistent latitudinal changes. It should be noted that VIC reproduces observed runoff quite well over the major river basins of both North America and Eurasia [*Su et al.*, 2005] which suggests that the VIC values, while they are not observations, are probably a reasonable surrogate. So we infer from this that ERA-40 most likely overestimates E, and underestimates R over the major Arctic river basins. Furthermore, the ERA-40 moisture convergence appears to be underestimated except for latitudes 45–50°N in Eurasia.

5. Summary

[41] This paper examines the land surface water fluxes from an off-line VIC simulation and ERA-40 reanalysis for the pan-Arctic land area. Observed P used to force the VIC model was compared to ERA-40 P. E-P calculated from the ERA-40 moisture flux convergence was used, with estimated P, to infer E, which was compared with ERA-40 and VIC E, and P-E was compared with runoff from VIC and ERA-40. The main findings of this study are as follows:

[42] 1. The annual means and monthly time series of ERA-40 P are in surprisingly (given uncertainty in the observations) good agreement with observations over the four largest Arctic basins. ERA-40 spatial patterns and latitudinal gradients are in general agreement with observations for both hemispheres. However, observed summer P is generally higher than ERA-40 P, especially in areas with high observed P. Averaged over the four large river basins, the differences between ERA-40 and observed P are probably within the error of observed P.

[43] 2. E has similar interannual, spatial, and latitudinal variations in the three estimates (VIC E, ERA-40 E, and implied E). The ERA-40 E shows higher values in annual means and in spring and autumn. The VIC model estimates more E in June and July than both the ERA-40 and atmospheric budgets most likely due to larger observed P than in ERA-40. The VIC E and implied E agree more closely during spring and autumn as compared to the ERA-40. Negative values of implied E in the southern Yenisei in summer and autumn reveal errors in the computed E-P.

[44] 3. The seasonal patterns of R in ERA-40 are poorly described in spite of its good representation of P. The problems of early snowmelt and two runoff peaks in the ERA-40 R indicate problems with the ECMWF land and snow schemes. Nonetheless, on an annual basis the spatial and latitudinal distributions of ERA-40 R are roughly consistent with the other estimates.

[45] 4. The long-term means of vapor convergence P-E for the Lena, Yenisei, Ob, and Mackenzie River basins are not balanced with the observed R, mainly due to the uncertainties in computed P-E and observed streamflow. The spatial and latitudinal distribution of annual P-E corresponds well with that of the VIC annual runoff, indicating some consistency between the surface water balance and the atmospheric moisture budget. However, locally where P-E is negative is an indication of errors in most cases. Nevertheless, convergence in one region has to be compensated for by divergence nearby and thus the area averages of P-E become more reliable.

[46] 5. The nonclosure terms are pretty small in the VIC over the four Arctic basins, while the surface water imbalances in ERA-40 account for 6%–27% of annual P due to the reanalysis increments. Most of the imbalances in the Ob (−62 mm) and Mackenzie (−119 mm) comes from the snow water increments in these two basins (−56 mm for the Ob, −88 mm for the Mackenzie).

[47] **Acknowledgments.** This work was supported by grants 0230372 and 0230327 to the University of Washington from the National Science Foundation, Office of Polar Programs. The authors would like to thank David Stepaniak and Lesley Smith at NCAR for computing the ERA-40 moisture budget fields. NCAR is sponsored by the National Science Foundation.

References

Aagaard, K., and E. C. Carmack (1989), The role of sea ice and other fresh waters in the Arctic circulation, *J. Geophys. Res.*, *94*(C10), 14,485–14,498.

Abdulla, F. A., D. P. Lettenmaier, E. F. Wood, and J. A. Smith (1996), Application of a macroscale hydrologic model to estimate the water

balance of the Arkansas-Red river basin, *J. Geophys. Res.*, *101*(D3), 7449–7459.
Adam, J. C., and D. P. Lettenmaier (2003), Adjustment of global gridded precipitation for systematic bias, *J. Geophys. Res.*, *108*(D9), 4257, doi:10.1029/2002JD002499.
Adam, J. C., E. A. Clark, D. P. Lettenmaier, and E. F. Wood (2006), Correction of global precipitation products for orographic effects, *J. Clim.*, *19*(1), 15–38.
Arora, V. K. (2001), Assessment of simulated water balance for continental-scale river basins in a AMIP 2 simulation, *J. Geophys. Res.*, *106*(D14), 14,827–14,842.
Arora, V. K., and G. J. Boer (2001), Effects of simulated climate change on the hydrology of major river basins, *J. Geophys. Res.*, *106*(D4), 3335–3348.
Barry, R. G., and M. C. Serreze (2000), Atmospheric components of the arctic ocean freshwater balance and their interannual variability, in *The Freshwater Budget of the Arctic Ocean*, edited by E. L. Lewis et al., pp. 45–56, Springer, New York.
Betts, A. K., and J. H. Ball (1999), Basin-scale surface water and energy budgets for the Mississippi from the ECMWF reanalysis, *J. Geophys. Res.*, *104*(D16), 19,293–19,306.
Betts, A. K., and P. Viterbo (2000), Hydrological budgets and surface energy balance of seven subbasins of the Mackenzie river from the ECMWF model, *J. Hydrometeorol.*, *1*, 47–60.
Betts, A. K., J. H. Ball, and P. Viterbo (2003a), Evaluation of the ERA-40 surface water budget and surface temperature for the Mackenzie river basin, *J. Hydrometeorol.*, *4*, 1194–1211.
Betts, A. K., J. H. Ball, M. Bosilovich, P. Viterbo, Y. Zhang, and W. B. Rossow (2003b), Intercomparison of water and energy budgets for five Mississippi subbasins between ECMWF reanalysis (ERA-40) and NASA Data Assimilation Office fvGCM for 1990–1999, *J. Geophys. Res.*, *108*(D16), 8618, doi:10.1029/2002JD003127.
Bowling, L. C., D. P. Lettenmaier, and B. V. Matheussen (2000), Hydroclimatology of the Arctic drainage basin, in *The Freshwater Budget of the Arctic Ocean: Proceedings of the NATO Advanced Research Workshop*, edited by E. L. Lewis et al., pp. 57–90, Springer, New York.
Bowling, L. C., et al. (2003), Simulation of high-latitude hydrological processes in the Torne-Kalix basin: PILPS Phase 2 (e): 1. Experiment description and summary intercomparisons, *Global Planet. Change*, *38*, 1–30.
Bras, R. A. (1990), *Hydrology, an Introduction to Hydrologic Science*, 643 pp., Addison-Wesley, Boston, Mass.
Cherkauer, K. A., and D. P. Lettenmaier (1999), Hydrologic effects of frozen soils in the upper Mississippi River basin, *J. Geophys. Res.*, *104*(D16), 19,599–19,610.
Cherkauer, K. A., and D. P. Lettenmaier (2003), Simulation of spatial variability in snow and frozen soil Field, *J. Geophys. Res.*, *108*(D22), 8858, doi:10.1029/2003JD003575.
Cullather, R. I., K. H. Bromwich, and M. C. Serreze (2000), The atmospheric hydrologic cycle over the Arctic basin from reanalyses. Part I: Comparison with observations and previous studies, *J. Clim.*, *13*, 923–937.
Dai, A., and K. E. Trenberth (2002), Estimates of freshwater discharge from continents: Latitudinal and seasonal variations, *J. Hydrometeorol.*, *3*, 660–687.
Gates, W. L. (1992), AMIP: The Atmospheric Model Intercomparison Project, *Bull. Am. Meteorol. Soc.*, *73*, 1962–1970.
Grabs, W. E., F. Portman, and T. de Couet (2000), Discharge observation networks in Arctic regions: Computation of the river runoff into the Arctic Ocean, its seasonality and variability, in *The Freshwater Budget of the Arctic Ocean*, edited by E. L. Lewis et al., pp. 249–267, Springer, New York.
Gutowski, W. J., Jr., Y. Chen, and Z. Ötles (1997), Atmospheric water vapor transport in NCEP-NCAR reanalysis: Comparison with river discharge in the central United States, *Bull. Am. Meteorol. Soc.*, *78*, 1957–1969.
Intergovernmental Panel on Climate Control (IPCC) (1995), *Climate Change 1995: The Science of Climate Change*, Cambridge Univ. Press, New York.
Kalnay, E., et al. (1996), The NCEP/NCAR 40-year reanalysis project, *Bull. Am. Meteorol. Soc.*, *77*, 437–471.
Kattsov, V. M., J. E. Walsh, A. Rinke, and K. Dethloff (2000), Atmospheric climate models: Simulation of the Arctic Ocean fresh water budget components, in *The Freshwater Budget of the Arctic Ocean: Proceedings of the NATO Advanced Research Workshop*, edited by E. L. Lewis et al., pp. 209–247, Springer, New York.
Kimball, J. S., S. W. Running, and R. R. Nemani (1997), An improved method for estimating surface humidity from daily minimum temperature, *Agric. For. Meteorol.*, *85*, 87–98.
Liang, X., D. P. Lettenmaier, E. Wood, and S. J. Burges (1994), A simple hydrologically based model of land surface water and energy fluxes for general circulation models, *J. Geophys. Res.*, *99*(D17), 14,415–14,428.
Liang, X., E. F. Wood, and D. P. Lettenmaier (1996), Surface soil moisture parameterization of the VIC-2L model: Evaluation and modifications, *Global Planet. Change*, *13*, 195–206.
Macdonald, R. W. (2000), Arctic estuaries and ice: A positive-negative estuarine couple, in *The Freshwater Budget of the Arctic Ocean*, edited by E. L. Lewis et al., pp. 383–407, Springer, New York.
Maurer, E. P., G. M. O'Donnel, D. P. Lettenmaier, and J. O. Roads (2001), Evaluation of the land surface water budget in NCEP/NCAR and NCEP/DOE reanalyses using an off-line hydrologic model, *J. Geophys. Res.*, *106*(D16), 17,841–17,862.
Maurer, E. P., A. W. Wood, J. C. Adam, and D. P. Lettenmaier (2002), A long-term hydrologically based dataset of land surface fluxes and states for the conterminous United States, *J. Clim.*, *15*, 3237–3251.
Moritz, R. E., C. M. Bitz, and E. J. Steig (2002), Dynamics of recent climate change in the Arctic, *Science*, *297*, 1497–1502.
Nijssen, B., G. M. O'Donnell, A. F. Hamlet, and D. P. Lettenmaier (2001a), Hydrologic vulnerability of global rivers to climate change, *Clim. Change*, *50*, 143–175.
Nijssen, B., R. Schnur, and D. P. Lettenmaier (2001b), Global retrospective estimation of soil moisture using the VIC land surface model, 1980–1993, *J. Clim.*, *14*(8), 1790–1808.
Oki, T., K. Musiake, H. Matsuyama, and K. Masuda (1995), Global atmospheric water balance and runoff from large river basins, *Hydrol. Processes*, *9*, 655–678.
Rawlins, M. A., R. B. Lammers, S. Frolking, B. M. Fekete, and C. J. Vorosmarty (2003), Simulating pan-arctic runoff with a macro-scale terrestrial water balance model, *Hydrol. Processes*, *17*, 2521–2539.
Roads, J. O., S.-C. Chen, A. K. Gueter, and K. P. Georgakakos (1994), Large-scale aspects of the United States hydrologic cycle, *Bull. Am. Meteorol. Soc.*, *75*, 1589–1610.
Rogers, A. N., D. H. Bromwich, E. N. Sinclair, and R. I. Cullather (2001), The atmospheric hydrologic cycle over the Arctic basin from reanalyses, 2, Interannual variability, *J. Clim.*, *14*, 2414–2429.
Ropelewski, C. F., and E. S. Yarosh (1998), The observed mean annual cycle of moisture budgets over the central United States (1973–92), *J. Clim.*, *11*, 2180–2190.
SEARCH SCC (2001), SEARCH: Study of Environmental Arctic Change, science plan, technical report, Polar Sci. Cent., Univ. of Wash., Seattle.
Seneviratne, S. I., P. Viterbo, D. Luthi, and C. Schar (2004), Inferring changes in terrestrial water storage using ERA-40 Reanalysis data: The Mississippi river basin, *J. Clim.*, *17*(11), 2039–2057.
Serreze, M. C., J. E. Walsh, F. S. Chapin III, T. Osterkamp, M. Dyurgerov, V. Romanovsky, W. C. Oechel, J. Morison, T. Zhang, and R. G. Barry (2000), Observational evidence of recent change in the northern high-latitude environment, *Clim. Change*, *46*, 159–207.
Serreze, M. C., D. H. Bromwich, M. P. Clark, A. J. Etringer, T. Zhang, and R. Lammers (2003), Large-scale hydro-climatology of the terrestrial Arctic drainage system, *J. Geophys. Res.*, *108*(D2), 8160, doi:10.1029/2001JD000919.
Serreze, M. C., A. Barrett, and F. Lo (2005), Northern high latitude precipitation as depicted by atmospheric reanalyses and satellite retrievals, *Mon. Weather Rev.*, *133*(12), 3407–3430.
Su, F., J. C. Adam, L. C. Bowling, and D. P. Lettenmaier (2005), Streamflow simulations of the terrestrial Arctic domain, *J. Geophys. Res.*, *110*, D08112, doi:10.1029/2004JD005518.
Thornton, P. E., and S. W. Running (1999), An improved algorithm for estimating incident daily solar radiation from measurements of temperature, humidity, and precipitatioin, *Agric. For. Meteorol.*, *93*, 211–228.
Trenberth, K. E. (1997), Using atmospheric budgets as constraint on surface fluxes, *J. Clim.*, *10*, 2796–2809.
Trenberth, K. E., and C. J. Guillemot (1995), Evaluation of the global atmospheric moisture budget as seen from analyses, *J. Clim.*, *8*, 692–708.
Trenberth, K. E., and C. J. Guillemot (1998), Evaluation of the atmospheric moisture and hydrological cycle in the NCEP/NCAR reanalyses, *Clim. Dyn.*, *14*, 213–231.
Trenberth, K. E., and L. Smith (2005), The mass of the atmosphere: A constrain on global analyses, *J.Clim.*, *18*, 864–875.
Uppala, S. M., et al. (2005), The ERA-40 reanalysis, *Q. J. R. Meteorol. Soc.*, *131*, 2961–3012, doi:10.1256/qj.04.176.
Van den Hurk, B., and P. Viterbo (2003), The Torne-Kalix PILPS 2 (e) experiment as a test bed for modifications to the ECMWF land surface scheme, *Global Planet. Change*, *38*, 165–173.
Van den Hurk, B., P. Viterbo, A. C. M. Beljaars, and A. K. Betts (2000), Offline validation of the ERA40 surface scheme, *ECMWF Tech. Memo. 295*, 43 pp., Eur. Cent. for Medium-Range Weather Forecasts, Reading, UK.

Vorosmarty, C. J., L. D. Hinzman, B. J. Peterson, D. H. Bromwich, L. C. Hamilton, J. Morison, V. E. Romanovsky, M. Sturm, and R. S. Webb (2001), The hydrologic cycle and its role in Arctic and global environmental change: A rationale and strategy for synthesis study, 84 pp., Arct. Res. Consortium of the U. S., Fairbanks, Alaska.

Walsh, J. E., V. Kattsov, D. Portis, and V. Meleshko (1998), Arctic precipitation and evapotranspiration: Model results and observational estimates, *J. Clim.*, *11*(1), 72–87.

Yeh, P. J. F., M. Irizarry, and E. A. B. Eltahir (1998), Hydroclimatology of Illinois: A comparison of monthly evapotranspiration estimates based on atmospheric water balance and soil water balance, *J. Geophys. Res.*, *103*(D16), 19,823–19,837.

J. C. Adam, D. P. Lettenmaier, and F. Su, Department of Civil and Environmental Engineering, University of Washington, Seattle, WA 98195-2700, USA. (fgsu@hydro.washington.edu)

K. E. Trenberth, National Center for Atmospheric Research, Boulder, CO 80307, USA.